HYDRODYNAMIC STABILITY IN AN ELECTROCHEMICAL CELL WITH A ROTATING DISK ELECTRODE: EFFECT OF A NON-STATIONARY VISCOSITY PROFILE

J. Pontes
Metallurgy and Materials Engineering Department – EE/COPPE/UFRJ
PO Box 68505, 21945-970 Rio de Janeiro RJ, Brazil
jopontes@ufrj.br

Norberto Mangiavacchi
Institute of Mathematical and Computational Sciences USP – S. Carlos,
PO Box 668, 13560-161 S.Carlos, SP, Brazil
norberto@icmc.sc.usp.br

Anderson R. Conceição
Metallurgy and Materials Engineering Department – EE/UFRJ
PO Box 68505, 21945-970 Rio de Janeiro RJ, Brazil
anderson@metalmat.ufrj.br

Rafael de Mattos Niederauer
Metallurgy and Materials Engineering Department – EE/UFRJ
PO Box 68505, 21945-970 Rio de Janeiro RJ, Brazil
rafael@wnetrj.com.br

Oswaldo E. Barcia
Institute of Chemistry – UFRJ,
PO Box 68505, 21945-970 Rio de Janeiro, Brazil
barcia@metalmat.ufrj.br

Oscar Rosa Mattos
Metallurgy and Materials Engineering Department – COPPE/UFRJ
PO Box 68505, 21945-970 Rio de Janeiro RJ, Brazil
omattos@metalmat.ufrj.br

Bernard Tribollet
UPR15 – CNRS, Physique des Liquides et Electrochimie,
4 place Jussieu, 75252 Paris Cedex 05, France
bt@ccr.jussieu.fr

Abstract. *P*olarization curves experimentally obtained in the electro-dissolution of iron in a 1 **M H_2SO_4** solution using a rotating disk as the working electrode present a current instability region within the range of applied voltage in which the current is controlled by mass transport in the electrolyte. According to the literature (Barcia *et. al*, 1992) the electro-dissolution process leads to the existence of an axial viscosity gradient in the interface metal-solution, which leads to a deviation from Von Kármán's classical solution for rotating disk flow. On four previous papers by Pontes *et al.* (2002a, 2002b, 2002c, 2003) they showed that the steady flow, affected by the viscosity gradient, is less stable than the constant viscosity flow with respect to disturbances with periodic variation along the radial direction and also, to spiral disturbances periodically varying along the radial and azimutal directions. No attempt has been made to take into account the transport of the relevant chemical species and to relate the viscosity gradient to the spatio-temporal distribution of those species. Therefore, an extension of the work developed up to now points to a stability analysis of the coupled hydrodynamic and chemical species fields, which will eventually show the existence of time dependent disturbances in the viscosity profile, affecting the overall stability properties of the problem. The purpose of this work is to advance a first step in this direction, not explicitly considering the transport of the chemical species, but by assuming that the viscosity profile is affected by perturbations in the hydrodynamic field. It is shown that the neutral stability curve obtained for a steady viscosity profile is modified by time-dependent disturbances in the viscosity profile and that both the magnitude and the phase angle between the perturbations of the viscosity profile and the hidrodynamic field affect the neutral curves.

The results presented support the hypothesis that the current oscillations observed in the polarization curve may originate from a hydrodynamic instability and point to the need of further studies, considering the stability of the coupled hydrodynamic and chemical species fields.

Keywords: *Rotating Disk Flow, Electrochemical Instabilities, Hydrodynamic Stability, Turbulence*

1. Introduction

Polarization curves experimentally obtained in the electro-dissolution of iron in a 1 **M** $\mathbf{H_2SO_4}$ solution using a rotating disk as the working electrode (see Fig. 1) present three different regions (Barcia *et. al*, 1992). The first region is associated with low over-voltages applied to the working electrode and the current is a function of the electric potential and dissolution process only. The electric current is controlled by the transfer of charges at the interface rotating disk/electrolyte solution, and the mass transport does not affect the electro-dissolution process. By increasing the applied potential, the curves show a second region where the hydrodynamic conditions, which depend on the angular velocity imposed to the rotating disk electrode, affect the rate of the anodic dissolution of iron. The current is a function of both the applied potential and the hydrodynamic field developed close to the rotating electrode. By further increasing the applied over-voltage a third region appears, where the current is totally controlled by mass-transport processes.

The polarization curves present a current plateau in this third region, defining a limit value for the current which depends on the hydrodynamic conditions set by the angular velocity of the electrode.

Two current instabilities are observed in the third region: one at the beginning of the current plateau and a second one at the end, where the electrode surface undergoes an active to passive transition (Ferreira *et. al*, 1994). The first instability is intrinsic to the system, while the current instability close to the active-passive transition is affected by the output impedance of the control equipment. This instability can be suppressed by using a negative feedback resistance (Epelboin, 1972), that gives rise to continuous curves. Barcia et. al. (1992) proposed that the electro-dissolution process leads to the existence of a viscosity gradient in the diffusion boundary layer, which modifies the steady velocity field close to the electrode and could affect the stability of the hydrodynamic field. On a previous paper, Pontes *et. al* (2002) showed that the steady flow, affected by the viscosity gradient, was less stable than the classical one, with respect to disturbances with periodic variation along the radial direction. On three subsequent papers by Pontes *et al.* (2002a, 2002b, 2003) they further indicated that the flow affected by the viscosity gradient was, in many cases, less stable to spiral disturbances, periodically varying along the radial and azimutal directions, than the constant viscosity flow studied by Malik (1986) and Lingwood (1995). No attempt has been made to consider the transport of the relevant chemical species and to relate the viscosity gradient to the spatio-temporal distribution of those species. Therefore, an extension of the work developed up to now should include the stability analysis of the coupled hydrodynamic and chemical species fields, and it is expected that this analysis will eventually show the existence of time dependent disturbances in the viscosity profile, affecting the overall stability properties of the problem. The purpose of this work is to advance one step in this way, not explicitly considering the transport of the chemical species, but by assuming that the viscosity profile is affected by perturbations in the velocity field. A time-dependent perturbation proportional to the axial component of the curl of the velocity perturbations is added to the steady viscosity profile and the effect of this perturbed profile on the overall stability of the hydrodynamic field is investigated. Time-dependent perturbations imposed to the viscosity profile are assumed to have a phase angle with respect to those imposed to the velocity field. Only stationary disturbances of the velocity field, namely, disturbances turning with the same angular velocity imposed to the disk are considered.

The paper is organized as follows: Section (2) describes the steady velocity flow, which is the problem base state, for the case of constant viscosity fluids and for one variable viscosity configuration. Section (3) deals with the linearized equations of the perturbed flow. Section (4) describes the numerical procedure used to evaluate the neutral curves. The Neutral curves are given in Sec. (5) and conclusions are presented in Sec. (6).

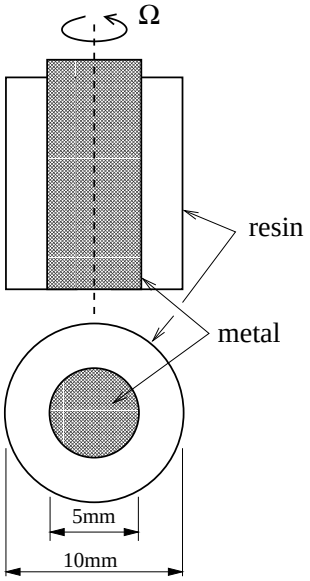

Fig. 1: The rotating disk electrode

2. The Base State

The steady hydrodynamic field is the well known Von Kármán (1921) exact solution of the continuity and Navier-Stokes equations for laminar rotating disk-flow, written in a rotating coordinate frame turning with the disk angular velocity Ω:

$$\mathbf{div}\,\mathbf{v} = 0 \tag{1}$$

$$\frac{D\mathbf{v}}{Dt} = -2\Omega \times \mathbf{v} - \frac{1}{\rho}\,\mathbf{grad}\,p + \frac{1}{\rho}\,\mathbf{div}\,\tau \tag{2}$$

where $-2\Omega \times \mathbf{v} = 2\Omega\,(v_\theta \mathbf{e}_r - v_r \mathbf{e}_\theta)$ and τ is the viscous stress tensor for a Newtonian fluid with the viscosity μ depending on the axial coordinate z. The components of stress tensor are given by (Schlichting, 1968):

$$\left.\begin{aligned} \tau_{rr} &= 2\mu\frac{\partial v_r}{\partial r} & \tau_{r\theta} &= \tau_{\theta r} = \mu\left(r\frac{\partial}{\partial r}\left(\frac{v_\theta}{r}\right) + \frac{1}{r}\frac{\partial v_r}{\partial \theta}\right) \\ \tau_{\theta\theta} &= 2\mu\left(\frac{1}{r}\frac{\partial v_\theta}{\partial \theta} + \frac{v_r}{r}\right) & \tau_{\theta z} &= \tau_{z\theta} = \mu\left(\frac{\partial v_\theta}{\partial z} + \frac{1}{r}\frac{\partial v_z}{\partial \theta}\right) \\ \tau_{zz} &= 2\mu\frac{\partial v_z}{\partial z} & \tau_{rz} &= \tau_{zr} = \mu\left(\frac{\partial v_r}{\partial z} + \frac{\partial v_z}{\partial r}\right) \end{aligned}\right\} \tag{3}$$

The steady solution takes the form:

$$\bar{v}_r = r\,\Omega\,F(\xi) \tag{4}$$

$$\bar{v}_\theta = r\,\Omega\,G(\xi) \tag{5}$$

$$\bar{v}_z = (\nu(\infty)\,\Omega)^{1/2}\,H(\xi) \tag{6}$$

$$\bar{p} = \rho\nu(\infty)\Omega P(\xi) \tag{7}$$

where $\xi = z(\Omega/\nu(\infty))^{1/2}$ and $\nu(\infty)$ is the bulk viscosity, far from the electrode surface. Equations (4–7) are introduced in the dimensional continuity and Navier-Stokes equations, leading to the following system of equations for F, G, H and P.

$$2F + H' = 0 \tag{8}$$

$$F^2 - (G+1)^2 + HF' = \frac{\partial}{\partial\xi}\left(\frac{\nu(\xi)}{\nu(\infty)}F'\right) \tag{9}$$

$$2F(G+1) + HG' = \frac{\partial}{\partial\xi}\left(\frac{\nu(\xi)}{\nu(\infty)}G'\right) \tag{10}$$

$$P' + HH' = 2\frac{\nu'(\xi)}{\nu(\infty)}H' + \frac{\nu(\xi)}{\nu(\infty)}H'' \tag{11}$$

Boundary conditions for F, G and H are $F = H = P = G = 0$ when $\xi = 0$, $F = H' = 0$, $G = -1$ when $\xi \longrightarrow \infty$. In order to integrate Eqs. (8–11) a viscosity profile must be assumed. In this work we use the following profile proposed by Barcia *et. al* (1992):

$$\frac{\nu(\xi)}{\nu(\infty)} = \frac{\nu(0)}{\nu(\infty)} + \left(1 - \frac{\nu(0)}{\nu(\infty)}\right)\frac{q^{1/3}}{\Gamma(4/3)}\int_0^\xi e^{-q\xi^3}\,d\xi \tag{12}$$

The parameter q defines the slope of the viscosity profile close to the electrode surface. Fig. 1 shows the rotating disk used in the experiments conducted by our group. This electrode consists of a $5\,mm$ diameter iron rod embedded in a $10\,mm$ diameter epoxy resin mold such that only its bottom cross section is allowed to contact the electrolyte. Figure 2 shows the non-dimensional viscosity and velocity profiles obtained by numerical integration of Eqs. (8–11) and used in the stability analysis presented in this work. The parameters assumed for the viscosity profile are $\nu(0)/\nu(\infty) = 6$ and $q = 2$.

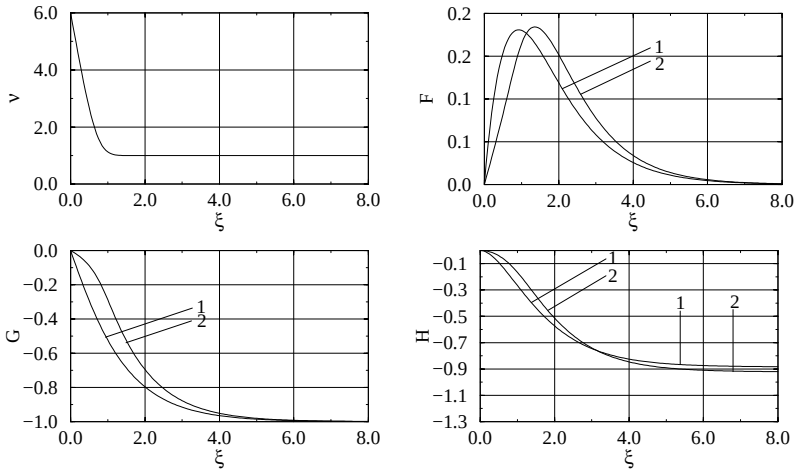

Fig. 2: Dimensionless viscosity, ν, and velocity profiles F, G and H. Curves No. 1 refer to constant viscosity fluids. Curves No. 2: variable viscosity fluids with $\nu(0)/\nu(\infty) = 6$ and $q = 2$ (see Eq. 12).

3. Perturbations of the Base State

We turn now to the question of the stability of the steady configurations of the hydrodynamic field described in Sec. (2), with respect to infinitesimally small disturbances. Variables in Eqs. (1–2) are made non-dimensional as follows: radial and axial coordinates are divided by the reference length $(\nu(\infty)/\Omega)^{1/2}$, velocity components are divided by the reference velocity $r_e^*\Omega$, pressure is divided by the reference pressure $\rho r_e^{*}\Omega^2$, viscosity is divided by the bulk value, $\nu^*(\infty)$ and time and the eigenvalue of the linearized problem are made non-dimensional using the factor $\nu(\infty)^{1/2}/(r_e^*\Omega^{3/2})$.

Here, r_e^* is the dimensional coordinate along the radial direction where the stability analysis is made. We define also the Reynolds number by the relation:

$$R = r_e^* \left(\frac{\Omega}{\nu(\infty)} \right)^{1/2} \tag{13}$$

The perturbed non-dimensional velocity components and pressure are written as:

$$v_r(t,r,\theta,\xi) = \frac{r}{R}F(\xi) + \tilde{v}_r(t,r,\theta,\xi) \tag{14}$$

$$v_\theta(t,r,\theta,\xi) = \frac{r}{R}G(\xi) + \tilde{v}_\theta(t,r,\theta,\xi) \tag{15}$$

$$v_z(t,r,\theta,\xi) = \frac{1}{R}H(\xi) + \tilde{v}_z(t,r,\theta,\xi) \tag{16}$$

$$p(t,r,\theta,\xi) = \frac{1}{R^2}P(\xi) + \tilde{p}(t,r,\theta,\xi) \tag{17}$$

$$\nu(t,r,\theta,\xi) = \bar{\nu}(\xi) + \tilde{\nu}(t,r,\theta,\xi) \tag{18}$$

Substituting the perturbed variables given by (14–17) in the non-dimensional continuity and Navier-Stokes equations and dropping nonlinear terms we obtain:

$$\frac{\tilde{v}_r}{r} + \frac{\partial \tilde{v}_r}{\partial r} + \frac{1}{r}\frac{\partial \tilde{v}_\theta}{\partial \theta} + \frac{\partial \tilde{v}_z}{\partial \xi} = 0 \tag{19}$$

$$\frac{\partial \tilde{v}_r}{\partial t} + \frac{r}{R}F\frac{\partial \tilde{v}_r}{\partial r} + \frac{G}{R}\frac{\partial \tilde{v}_r}{\partial \theta} + \frac{H}{R}\frac{\partial \tilde{v}_r}{\partial \xi} + \frac{F}{R}\tilde{v}_r - \frac{2}{R}(G+1)\tilde{v}_\theta + \frac{r}{R}F'\tilde{v}_z = -\frac{\partial \tilde{p}}{\partial r} +$$
$$\frac{\bar{\nu}}{R}\left(\frac{\partial^2 \tilde{v}_r}{\partial r^2} + \frac{1}{r^2}\frac{\partial^2 \tilde{v}_r}{\partial \theta^2} + \frac{\partial^2 \tilde{v}_r}{\partial \xi^2} + \frac{1}{r}\frac{\partial \tilde{v}_r}{\partial r} - \frac{2}{r^2}\frac{\partial \tilde{v}_\theta}{\partial \theta} - \frac{\tilde{v}_r}{r^2} \right) + \tilde{\nu}\frac{r}{R^2}F'' + \frac{\bar{\nu}'}{R}\left(\frac{\partial \tilde{v}_z}{\partial r} + \frac{\partial \tilde{v}_r}{\partial \xi} \right) + \frac{r}{R^2}F'\frac{\partial \tilde{\nu}}{\partial \xi} + 2\frac{F}{R^2}\frac{\partial \tilde{\nu}}{\partial r} \tag{20}$$

$$\frac{\partial \tilde{v}_\theta}{\partial t} + \frac{r}{R}F\frac{\partial \tilde{v}_\theta}{\partial r} + \frac{G}{R}\frac{\partial \tilde{v}_\theta}{\partial \theta} + \frac{H}{R}\frac{\partial \tilde{v}_\theta}{\partial \xi} + \frac{F}{R}\tilde{v}_\theta + \frac{2}{R}(G+1)\tilde{v}_r + \frac{r}{R}G'\tilde{v}_z = -\frac{1}{r}\frac{\partial \tilde{p}}{\partial \theta} +$$
$$\frac{\bar{\nu}}{R}\left(\frac{\partial^2 \tilde{v}_\theta}{\partial r^2} + \frac{1}{r^2}\frac{\partial^2 \tilde{v}_\theta}{\partial \theta^2} + \frac{\partial^2 \tilde{v}_\theta}{\partial \xi^2} + \frac{1}{r}\frac{\partial \tilde{v}_\theta}{\partial r} + \frac{2}{r^2}\frac{\partial^2 \tilde{v}_r}{\partial \theta^2} - \frac{\tilde{v}_\theta}{r^2} \right) + \tilde{\nu}\frac{r}{R^2}G'' + \frac{\bar{\nu}'}{R}\left(\frac{1}{r}\frac{\partial \tilde{v}_z}{\partial \theta} + \frac{\partial \tilde{v}_\theta}{\partial \xi} \right) + \frac{r}{R^2}G'\frac{\partial \tilde{\nu}}{\partial \xi} + 2\frac{F}{R^2}\frac{\partial \tilde{\nu}}{\partial \theta} \tag{21}$$

$$\frac{\partial \tilde{v}_z}{\partial t} + \frac{r}{R}F\frac{\partial \tilde{v}_z}{\partial r} + \frac{G}{R}\frac{\partial \tilde{v}_z}{\partial \theta} + \frac{H}{R}\frac{\partial \tilde{v}_z}{\partial \xi} + \frac{H}{R}\tilde{v}_z = -\frac{\partial \tilde{p}}{\partial \xi} +$$
$$\frac{\bar{\nu}}{R}\left(\frac{\partial^2 \tilde{v}_z}{\partial r^2} + \frac{1}{r^2}\frac{\partial^2 \tilde{v}_z}{\partial \theta^2} + \frac{\partial^2 \tilde{v}_z}{\partial \xi^2} + \frac{1}{r}\frac{\partial \tilde{v}_z}{\partial r} \right) + \frac{\tilde{\nu}}{R}\left(2\frac{F"}{R^2} + \frac{2H''}{R^2} \right) + 2\frac{\bar{\nu}'}{R}\frac{\partial \tilde{v}_z}{\partial \xi} + 2\frac{\partial \tilde{\nu}}{\partial \xi}\frac{H'}{R^2} + \frac{r}{R^2}F'\frac{\partial \tilde{\nu}}{\partial r} + \frac{G'}{R^2}\frac{\partial \tilde{\nu}}{\partial \theta} \tag{22}$$

At this stage we assume that the perturbation variables are separable and look for a solution in the form:

$$\begin{pmatrix} \tilde{v}_r \\ \tilde{v}_\theta \\ \tilde{v}_z \\ \tilde{p} \\ \tilde{\nu} \end{pmatrix} = \begin{pmatrix} f(\xi) \\ g(\xi) \\ h(\xi) \\ \pi(\xi) \\ \psi\,\eta(\xi) \end{pmatrix} \exp[i(\alpha r + \beta R\theta - \omega t)] \tag{23}$$

where $\eta = \alpha g - \beta f$, ψ and ω are complex numbers, with $\Re(\omega)$ and $\Im(\omega)$ being, respectively, the frequency and the rate of growth of the perturbation. Parameters α and β are the components of the perturbation wave-vector along the radial and azimuthal directions. For a given time, the phase of the perturbation is constant along branches of a logarithm spiral, with the branches curved in the clockwise direction if β is positive and counter-clockwise, if negative. Substitution of the perturbation variables in Eqs. (19–22) leads to:

$$i\left(\alpha - \frac{i}{r}\right)f + i\frac{R}{r}\beta g + h' = 0 \tag{24}$$

$$i\left(\frac{r}{R}\alpha F + \beta G - \omega\right)f + \frac{r}{R}F'h + i\alpha\pi = \frac{1}{R}\left(\nu f'' - \nu\left(\alpha^2 + \frac{R^2}{r^2}\beta^2\right)f - Ff + 2(G+1)g -\right.$$
$$\left. Hf' + i\alpha\nu'h + \nu' f'\right) + \frac{1}{R^2}\left(i\frac{R}{r}\nu\alpha f - 2\,i\frac{R^2}{r^2}\nu\beta g\right) - \frac{\nu}{Rr^2}f + \frac{\psi F'}{R}\eta' + \psi\frac{F''}{R}\eta + 2i\alpha\psi\frac{F}{R^2}\eta \tag{25}$$

$$i\left(\frac{r}{R}\alpha F + \beta G - \omega\right)g + \frac{r}{R}G'h + i\frac{R}{r}\beta\pi = \frac{1}{R}\left(\nu g'' - \nu\left(\alpha^2 + \frac{R^2}{r^2}\beta^2\right)g - Fg + 2(G+1)f -\right.$$
$$\left. Hg' + i\frac{R}{r}\beta\nu'h + \nu' g'\right) + \frac{1}{R^2}\left(i\frac{R}{r}\nu\alpha g - 2\,i\frac{R^2}{r^2}\nu\beta f\right) - \frac{\nu}{Rr^2}g + \frac{\psi G'}{R}\eta' + \psi\frac{G''}{R}\eta + 2i\beta\psi\frac{F}{R^2}\eta \tag{26}$$

$$i\left(\frac{r}{R}\alpha F + \beta G - \omega\right)h + \pi' = \frac{1}{R}\left(\nu h'' - \nu\left(\alpha^2 + \frac{R^2}{r^2}\beta^2\right)h - Hh' - H'h + 2\,\nu' h'\right) + \frac{i}{Rr}\,\nu\alpha h +$$
$$2\psi\frac{H'}{R^2}\eta' + 2\psi\frac{1}{R^2}\left(F' + H''\right)\eta + i\psi\frac{1}{R}\left(\alpha F" + \beta G"\right)\eta \tag{27}$$

where $\lambda^2 = \alpha^2 + \beta^2$. Equations (24–27) show that perturbation variables are not, strictly speaking, separable. In order to overcome the problem it is necessary to make the *parallel flow* assumption, usually adopted in stability analysis of growing boundary layers, where variations of the Reynolds number in the stream-wise direction are ignored. Adoption of this hypothesis in rotating disk flow (Malik,1981, 1986, Wilkinson and Malik, 1985, Lingwood, 1995) is made by replacing r by R in Eqs. (24-27):

$$i\left(\alpha - \frac{i}{R}\right) f + i\beta g + h' = 0 \tag{28}$$

$$i\left(\alpha F + \beta G - \omega\right) f + F'h + i\alpha\pi = \frac{1}{R}\left(\nu f'' - \nu\lambda^2 f - Ff + 2(G+1)g - Hf' + i\alpha\nu' h + \nu' f'\right) + \frac{1}{R^2}\left(i\nu\alpha f - 2\,i\nu\beta g\right) - \frac{\nu}{R^3} f + \frac{\psi F'}{R}\eta' + \psi\frac{F''}{R}\eta + 2i\alpha\psi\frac{F}{R^2}\eta \tag{29}$$

$$i\left(\alpha F + \beta G - \omega\right) g + G'h + i\beta\pi = \frac{1}{R}\left(\nu g'' - \nu\lambda^2 g - Fg + 2(G+1)f - Hg' + i\beta\nu' h + \nu' g'\right) + \frac{1}{R^2}\left(i\nu\alpha g - 2\,i\nu\beta f\right) - \frac{\nu}{R^3} g + \frac{\psi G'}{R}\eta' + \psi\frac{G''}{R}\eta + 2i\beta\psi\frac{F}{R^2}\eta \tag{30}$$

$$i\left(\alpha F + \beta G - \omega\right) h + \pi' = \frac{1}{R}\left(\nu h'' - \nu\lambda^2 h - Hh' - H'h + 2\,\nu' h'\right) + \frac{i}{R^2}\nu\alpha h + 2\psi\frac{H'}{R^2}\eta' + 2\psi\frac{1}{R^2}\left(F' + H''\right)\eta + i\psi\frac{1}{R}\left(\alpha F" + \beta G"\right)\eta \tag{31}$$

Equations 28–31 reduce to Eqs. 2.16–2.19 given by Malik (1986), in the case of constant viscosity fluids ($\nu = 1,\ \nu' = \nu'' = 0$). By eliminating π, neglecting terms of order R^{-2} and defining $D^n = d^n/d\xi^n$, $\bar{\alpha} = \alpha - i/R$ and $\bar{\lambda}^2 = \alpha\bar{\alpha} + \beta^2$ we obtain a sixth order system of two coupled equations in the form:

$$\left(i\nu\left(D^2 - \lambda^2\right)\left(D^2 - \bar{\lambda}^2\right) + i\nu' D\left(2D^2 - \lambda^2 - \bar{\lambda}^2\right) + i\nu''\left(D^2 + \bar{\lambda}^2\right) + R\left(\alpha F + \beta G - \omega\right)\left(D^2 - \bar{\lambda}^2\right) - R\left(\bar{\alpha}F'' + \beta G''\right) - iHD\left(D^2 - \bar{\lambda}^2\right) - iH'\left(D^2 - \bar{\lambda}^2\right) - iFD^2\right) h + \left(2\left(G+1\right)D + 2G' + \psi\left(\bar{\alpha}F''' + \beta G'''\right) + \psi\bar{\lambda}^2\left(\alpha F' + \beta G'\right) + \psi\left(\bar{\alpha}F' + \beta G'\right)D^2 + 2\psi\left(\bar{\alpha}F'' + \beta G''\right)D\right)\eta = 0 \tag{32}$$

$$\left(2\left(G+1\right)D - iR\left(\alpha G' - \beta F'\right)\right) h + \left(i\nu\left(D^2 - \lambda^2\right) + i\nu' D + R\left(\alpha F + \beta G - \omega\right) - iHD - iF + i\psi\left(\alpha G' - \beta F"\right)D + i\psi\left(\alpha G'' - \beta F''\right)\right)\eta = 0 \tag{33}$$

Equations 33–33 reduce to Eqs. 2.20–2.21 given by Malik (1986), in the case of constant viscosity fluids and are now rewritten in the form:

$$\begin{pmatrix} a_4D^4 + a_3D^3 + a_2D^2 + a_1D + a_0; & b_2D^2 + b_1D + b_0 \\ c_1D + c_0; & d_2D^2 + d_1D + d_0 \end{pmatrix}\begin{pmatrix} h \\ \eta \end{pmatrix} = \omega\begin{pmatrix} q_2D^2 + q_0; & 0 \\ 0; & s_0 \end{pmatrix}\begin{pmatrix} h \\ \eta \end{pmatrix} \tag{34}$$

with the coefficients given by:

$$a_4 = i\nu \qquad a_3 = i(2\nu' - H)$$
$$a_2 = i\nu'' - i\nu\left(\lambda^2 + \bar{\lambda}^2\right) + R\left(\alpha F + \beta G\right) - i\left(H' + F\right)$$
$$a_1 = -i\nu'\left(\lambda^2 + \bar{\lambda}^2\right) + iH\bar{\lambda}^2$$
$$a_0 = i\bar{\lambda}^2\left(\nu'' + \nu\lambda^2\right) - R\left(\alpha F + \beta G\right)\bar{\lambda}^2 - R\left(\bar{\alpha}F'' + \beta G''\right) + iH'\bar{\lambda}^2$$
$$b_2 = \psi\left(\bar{\alpha}F' + \beta G'\right) \qquad b_1 = 2\left(G+1\right) + 2\psi\left(\bar{\alpha}F'' + \beta G''\right)$$
$$b_0 = 2G' + \psi\left(\bar{\alpha}F''' + \beta G'''\right) + \psi\bar{\lambda}^2\left(\alpha F' + \beta G'\right)$$
$$c_1 = 2\left(G+1\right) \qquad c_0 = -iR\left(\alpha G' - \beta F'\right)$$
$$d_2 = i\nu \qquad d_1 = i\left(\nu' - H\right) + i\psi\left(\alpha G' - \beta F"\right)$$
$$d_0 = -i\nu\lambda^2 + R\left(\alpha F + \beta G\right) - iF + i\psi\left(\alpha G'' - \beta F''\right)$$
$$q_2 = R \qquad q_0 = -R\bar{\lambda}^2 \qquad s_0 = R$$

Eq. (34) defines a generalized eigenvalue/eigenfunction problem. The eigenfunctions are the normal modes of the model, the imaginary and real parts of each eigenvalue being, respectively, the rate of growth and the angular velocity of the perturbation relative to the angular velocity of the disk. Positive $\Re(\omega)$ means perturbations that turn with angular velocity smaller than the disk velocity, while negative $\Re(\omega)$ means perturbations that turn faster than the disk.

For a given viscosity profile the parameter space of the problem contains *three* variables, the Reynolds number and the perturbation wave-vector components α and β.

Boundary conditions of the problem require non-slip flow and vanishing axial component of the velocity at the electrode surface. These conditions are already fulfilled by the base-state, so the hydrodynamic field cannot be modified by the perturbation at the electrode surface. In consequence we must require $g = h = 0$ in $\xi = 0$. Moreover, we conclude from Eq. (24) that $h' = 0$ at the electrode surface. In $\xi \longrightarrow \infty$ we require that the perturbation vanishes ($g = h = 0$) and that $h' = 0$.

4. Numerical Procedure

The numerical precedure consists of finding the neutral stability curves ($\Im(\omega) = 0$) in the space of parameters α, β and R, for stationary perturbations turning with the angular velocity of the disk $\Re(\omega) = \omega_p = 0$.

Building the neutral curves requires finding the set of points $c(s) = (\alpha(s), \beta(s), R(s))$ that satisfy $F(c(s)) = 0$, where $F : R^3 -> R^2$ is given by $F = (\Im(\omega), \Re(\omega) - \omega_p)^T$. The neutral curves are built using a Predictor-Corrector Continuation method described in E. Allgower, K. Georg (1991). Here, for completeness, we will give a short description of the employed method:

- The perturbation frequency ω_p is specified and an initial point c_0, in the parameters space α, β, R is given. This point is not necessarily on the neutral curve;
- This initial point is corrected using an inexact Newton iteration given by

$$c_i^{n+1} = c_i^n - F'(c_i^0)^+ F(c_i^n) \tag{35}$$

  where $F'(v_0)^+$ is the pseudo-inverse of Moore-Penrose of the Jacobian of F. The Jacobian is computed numerically, using a finite difference approximation.
- To obtain a new point, first a Predictor step is employed, using a first order Euler approximation:

$$c_{i+1}^0 = c_i + h\ t(F'(c_i)) \tag{36}$$

  where h is a suitable step size, and $t(F'(c_i))$ is the tangent vector to curve $c(s)$.
- The value c_{i+1}^0 is corrected in a Corrector step using Eq. (35) iteratively until a satisfactorily converged value is obtained.
- The solution of the generalized eigenvalue/eigenfunction problem required to evaluate $F(c(s))$ is obtained numerically, using an efficient implementation of the Inverse Power Method for complex generalized non-symmetric eigenproblems.

Validation of the numerical procedure is described in the paper by Pontes *et al.* (2002b).

5. Results

The purpose of this work is to perform a numerical investigation on the effect of a time-dependent perturbation imposed to a given viscosity profile, on the neutral curve of stationary disturbances in rotating disk flow with a steady viscosity profile according to Eq.(12), with $\nu(0)/\nu(\infty) = 6$ and $q = 2$.

For the sake of comparison, we present first the neutral curves of stationary disturbances, for constant viscosity fluids and for fluids with the steady viscosity profile, already given by Pontes *et al.* (2002b, 2003). These curves are presented in Fig. (3) and the destabilizing effect of the steady viscosity profile is clear.

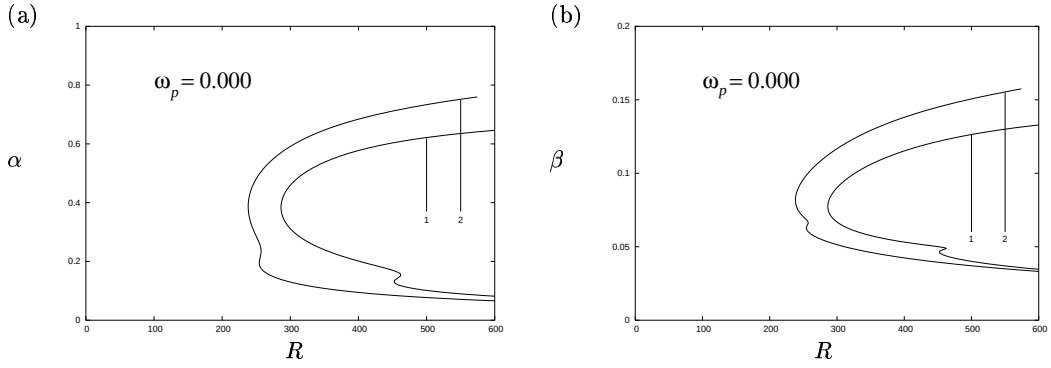

Fig. 3: Neutral curves in the $R \times \alpha$ and $R \times \beta$ planes for stationary disturbances ($\Re(\omega) = 0$) in constant viscosity flows (curves No. 1) and variable viscosity fluids (curves No. 2) with $\nu(0)/\nu(\infty) = 6.0$ and $q = 2.00$ (see Eq. 12).

We now turn to the effect of imposing a perturbation to the steady viscosity profile in the form $\psi\eta$, on the neutral curve No. 2 shown in Fig. (3). Values assigned to ψ are ± 1, ± 1.5, $\pm i$ and $\pm 1.5i$. The neutral curves were evaluated in domains with length $\xi_{max} = 25$ and grids with 501 points uniformly spaced. The results are presented in Fig. (4) and briefly summarized below.

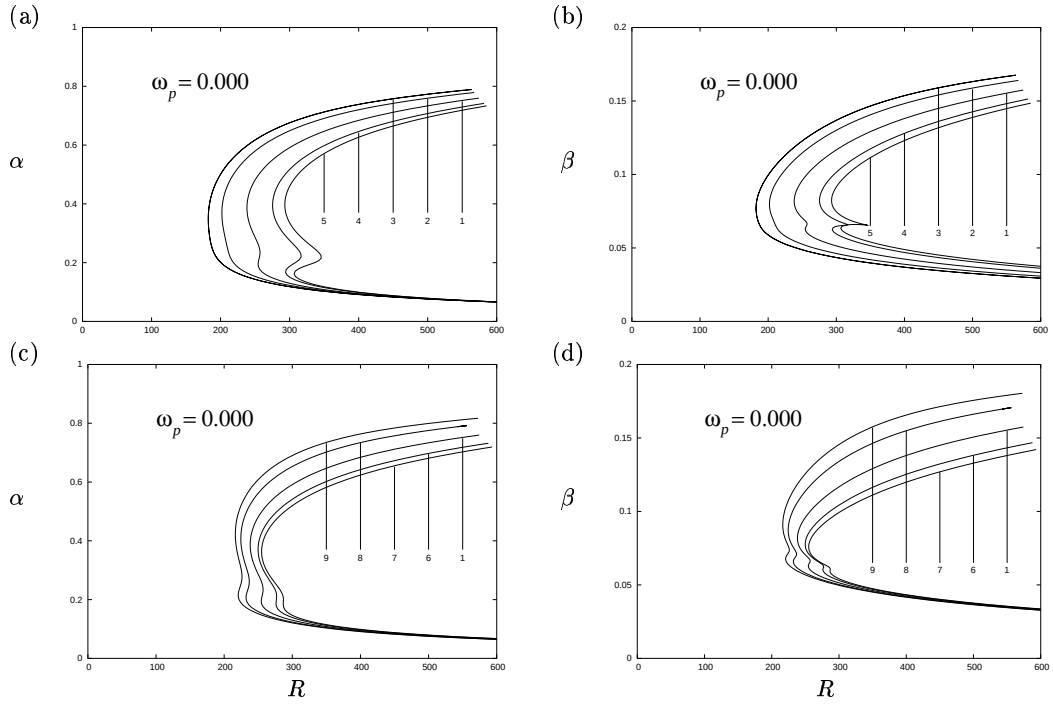

Fig. 4: Neutral curves in the $R \times \alpha$ and $R \times \beta$ planes for stationary disturbances ($\Re(\omega) = 0$) in variable viscosity fluids with $\nu(0)/\nu(\infty) = 6.0$ and $q = 2.00$ (see Eq. 12). Curves No. 1 refer to steady viscosity profiles; Curves No. 2: $\psi = 1.0$; Curves No. 3: $\psi = 1.5$; Curves No. 4: $\psi = -1.0$; Curves No. 5: $\psi = -1.5$; Curves No. 6: $\psi = 1.0i$; Curves No. 7: $\psi = 1.5i$; Curves No. 8: $\psi = -1.0i$; Curves No. 9: $\psi = -1.5i$.

Diagrams (a) and (b) compare the neutral curve obtained for a steady viscosity profile (curve No. 1), with those obtained with $\psi = 1.0$ (curve No. 2), $\psi = 1.5$ (curve No. 3), $\psi = -1.0$ (curve No. 4) and $\psi = -1.5$ (curve No. 5). From these curves we conclude that perturbations of the viscosity profile in phase with η, the vertical component of the curl of the velocity perturbations, render the flow less stable. Larger perturbations imposed to the viscosity profile lead to neutral curves with lower critical Reynolds numbers. On the other extreme, when perturbations in opposite phase with η ($\psi = -1.0$ and -1.5) are imposed to the viscosity profile, a stabilizing effect is observed and larger magnitudes of the perturbation applied to the viscosity profile result in larger stabilizing effects.

Diagrams (c) and (d) in Fig. (4) compare the neutral curve obtained for a stready viscosity profile (curve No. 1), with those obtained when the phase angle between perturbations applied to the viscosity profile and η are $\pm\pi/2$. These diagrams show that perturbations with a phase angle of $-\pi/2$ render the flow less stable than the one obtained with a steady viscosity profile and that this effect increases if larger magnitudes of the perturbation are imposed to that profile.

Table 1: Approximate coordinates of the absolute minimum of the neutral curves shown in Figs. 3, 4 and 5.

ψ	R	α	β
$\nu = $ Const.	286.3	0.38482	0.07753
0	239.4	0.38577	0.08158
1.0	201.9	0.36614	0.07932
$-1.0i$	224.4	0.40842	0.08737
$1.0i$	249.7	0.37341	0.07801
-1.0	275.4	0.40241	0.08334
1.5	182.2	0.34971	0.07720
$-1.5i$	216.4	0.41849	0.09040
$1.5i$	254.9	0.36004	0.07546
-1.5	293.0	0.39372	0.08189

An opposite effect is observed for perturbations forming a phase angle of $\pi/2$ with η: the flow becomes more stable and the stabilizing effect increases if perturbations with larger magnitude are applied to the viscosity profile.

Figure (5) shows the effect of the phase angle between the viscosity profile perturbation and η for $|\psi| = 1$. This figure shows that viscosity perturbations in phase with η ($\psi = 1.0$) result in the largest destabilizing effect, followed by those with a phase angles of $-\pi/2$ ($\psi = i$), $\pi/2$ ($\psi = -i$), and π ($\psi = -1.0$), the with the last two playing stabilizing roles.

Coordinates of the absolute minimum of the neutral curves presented in this work are given in Table 1.

6. Conclusions

In conclusion we further analyzed the Pontes *et al.'s* (2002a, 2002b, 2002c, 2003) previous stability work of rotating disk flows in electrochemical cells, where the fluid viscosity varies

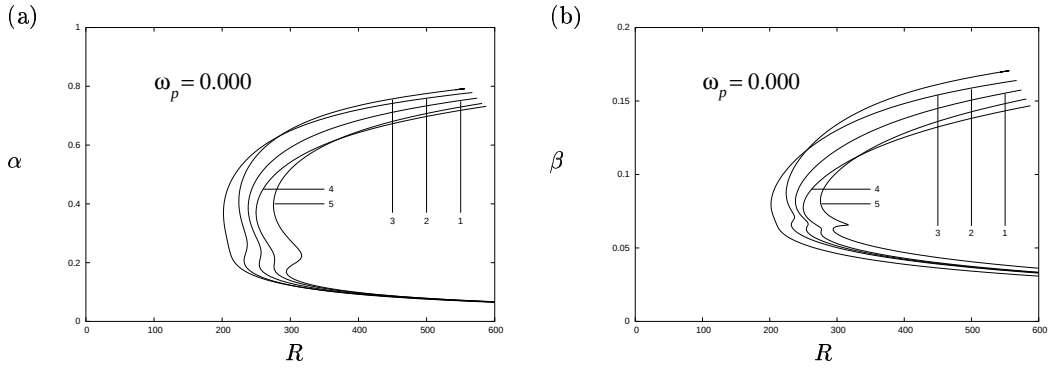

Fig. 5: Neutral curves in the $R \times \alpha$ and $R \times \beta$ planes for stationary disturbances ($\Re(\omega) = 0$) in variable viscosity fluids with $\nu(0)/\nu(\infty) = 6.0$ and $q = 2.00$ (see Eq. 12). Curves No. 1 refer to steady viscosity profiles. Curves No. 2: $\psi = 1.0$; Curves No. 3: $\psi = -i$; Curves No. 4: $\psi = i$; Curves No. 5: $\psi = -1.0$

along the axis of the rotating electrode. Previous analysis did not take into account the coupling between the chemical species and the hydrodynamic fields. So, the purpose of this work was having a first insight on the result of this coupling, by investigating the effect of adding a time-dependent perturbation to the viscosity profile. Perturbations proportional to η, the vertical component of the curl of the velocity perturbation were added to the steady viscosity profile and the evolution of the perturbed flow was investigated by means of temporal linear analysis. The results indicate that the neutral curve is more affected by time-dependent perturbations of larger magnitudes introduced in the viscosity profile but both stabilizing and destabiling effects were observed, dependig on the phase angle between the perturbation applied to the viscosity profile and the velocity perturbation. These results suggest that the actual neutral curves may deviate from those obtained on the assumption of steady viscosity profiles and point to the need of extending the analysis carried up to now in order to take into account the coupling of the hydrodynamic and chemical species fields, through the dependency of the viscosity with the concentration of the relevant chemical species.

7. Acknowledgments

The authors acknowledge prof. Antônio Castelo Filho (USP-S.Carlos, Brazil), who developed the numerical code using the Continuation Method to evaluate the neutral stability curves presented in this work. J. P. acknowledges financial support received from FAPERJ (Brazil) under the contract number E-26/171.300/2001.

8. References

Barcia, O. E., Mattos, O. R., and Tribollet, B., 1992, Anodic dissolution of iron in acid sulfate under mass transport control, "J. Eletrochem. Soc.", Vol. 139, pp. 446–453.

Ferreira, J. R. R. M., Barcia, O. E., and Tribollet, B., 1994, Iron dissolution under mass transport control: the effect of viscosity on the current oscillation, "Eletrochim. Acta", Vol. 39, pp. 933–938.

Lingwood, R. J., 1995, Absolute instability of the boundary layer on a rotating disk, "J. Fluid Mech.", Vol. 299, pp. 17–33.

Malik, M. R., 1986, The Neutral Curve for Stationary Disturbances in Rotating-disk Flow, "J. Fluid Mech.", Vol. 164, pp. 275–287.

Malik, M. R., Wilkinson, and Orzag, S. A., 1981, Instability and Transition in a Rotating Disk, "AIAA J.", Vol. 19-9, pp. 1131–1138.

Pontes, J., Mangiavacchi, N., Conceição, A. R., Barcia, O. E., Mattos, O. E., and Tribollet, B., 2002a, Instabilities in Electrtochemical Systems with a Rotatinng Disk electrode, "J. of the Braz. Soc. of Mechanical Sciences", Vol. XXIV-3, pp. 139–148.

Pontes, J., Mangiavacchi, N., Conceição, A. R., Barcia, O. E., Mattos, O. R., and Tribollet, B., 2002b, Hydrodynamic Stability in an Electrochemical Cell with a Rotating Disk Electrode, "Proceedings of the 9^{th} Brazilian Congress of Thermal Engineering and Sciences", Caxambu, MG, Brazil. paper CIT02-0125 (in CD).

Pontes, J., Mangiavacchi, N., Conceição, A. R., Barcia, O. E., Mattos, O. R., and Tribollet, B., 2002c, Rotating Disk Flow Stability in Eletrochemical Cells, "Anais da III Escola Brasileira de Primavera Transição e Turbulência", Florianópolis, SC, Brazil. (in CD).

Pontes, J., Mangiavacchi, N., Conceição, A. R., Barcia, O. E., Mattos, O. R., and Tribollet, B., 2003, Rotating Disk Flow Stability in Electrochemical Cells: Effect of Fluid Viscosity, submitted, Phys. Fluids.

Schlichting, H. and Gersten, K., 2000, "Boundary Layer Theory", Springer.

von Kármán, T. and Angew, Z., 1921, Uber Laminare und Turbulente Reibung, "Math. Mec.", Vol. 1, pp. 233–252.

Wilkinson, s. and Malik, M. R., 1985, Stability Experiments in the Flow Over a Rotating Disk, "AIAA J.", Vol. 23, pp. 588.